The influence of H_2O or/and O_2 introduction during the low-temperature gas-phase sulfation of organic $COS+CS_2$ on the conversion and deposition of sulfur-containing species in the sulfated CeO_2-OS catalyst for NH_3-SCR

Zhibo Xiong[1*], Yafei Zhu[1], Jiaxing Liu[1], Yanping Du[2], Fei Zhou[3], Jing Jin[1**], Qiguo Yang[1**], Wei Lu[1]

1. School of Energy and Power Engineering, University of Shanghai for Science & Technology, Shanghai, 200093, China

2. School of Engineering, Lancaster University, Lancaster, LA1 4YW, UK

3. Jiangsu Guoxin Jingjiang Power Co. Ltd., Jingjiang 214500, Jiangsu, China

Abstract:

Herein, the typical components of blast furnace gas, including H_2O and O_2, were introduced to improve the NH_3-SCR activity of the sulfated CeO_2-OS catalyst during the gas-phase sulfation of organic $COS+CS_2$ at 50 °C. The characterization results demonstrate that the introduction of O_2 or H_2O during the gas-phase sulfation enhances the conversion of organic $COS+CS_2$ on cubic fluorite CeO_2 surface and reduces the formation of sulfur and sulfates in catalyst, but decreases the BET surface area and pore volume of CeO_2-OS. However, the introduction of O_2 or H_2O during the gas-phase sulfation increases the molar ratios of $Ce^{3+}/(Ce^{3+}+Ce^{4+})$ and $O_\beta/(O_\alpha+O_\beta+O_\gamma)$ on the CeO_2-OS catalyst surface, thus promotes the formation of surface oxygen vacancies and chemisorbed oxygen, and these properties of catalyst are further enhanced by the co-existence of O_2 and H_2O. Furthermore, the reduction of the formed sulfates under the action of O_2 or H_2O decreases the weak acid sites of CeO_2-OS catalyst, but the less and highly dispersive sulfates presents stronger reducibility and the proportion of medium-strong acid sites of catalyst increases. These all help to improve the NH_3-SCR activity of CeO_2-OS catalyst. Therefore, there exists a synergistic effect of H_2O and O_2 introduction during the gas-phase sulfation on the physical-chemical properties and catalytic performance of the sulfated CeO_2-OS catalyst by organic $COS+CS_2$ at 50 °C.

Keywords: NH_3-SCR, CeO_2, gas-phase sulfation, Organic sulfur, hydrolysis temperature, O_2/H_2O, Sulfur-containing species, Regulation

* Corresponding author: Zhibo Xiong, Tel.: +86 21 55272320, Email addresses: xzb412@usst.edu.cn (Z.Xiong)

** Corresponding author: Jing Jin, Qiguo Yang, Email addresses: alicejin001@163.com(J. Jin), yangqg@usst.edu.cn (Q. Yang).

1. Introduction

The emission of industrial pollutants from the utilization of fossil fuels, including organic sulfur (COS, CS_2 and CH_3SH, etc.) and nitrogen oxides (NO, NO_2 and N_2O, etc.), cause serious environmental pollution problems, including acid rain, photochemical smog and so on, which also brings serious harm to human health. For example, long-term exposure to CS_2 increases the risk of cardiovascular disease and damages the hearing system, while nitrogen oxides triggers throat irritation and increases the likelihood of respiratory diseases.[1-5] Therefore, strict standards and policies have been implemented worldwide to reduce the emission of sulfur-containing compounds and nitrogen oxides.[6]

Carbonyl sulfide (COS) and carbon disulfide (CS_2) are the main components of organosulfur compounds and have similar triatomic linear spatial configuration of CO_2 molecule, which are difficult to be removed due to the stable chemical properties.[7,8] At present, the technologies of cold methanol washing, uptake/adsorption, oxidation and photolysis have been proposed to reduce organic COS and CS_2, but the defects of low removal efficiency, harsh reaction conditions and complex regeneration process hampered their large-scale application. Meanwhile, catalytic hydrolysis has been found to reduce COS or/and CS_2 under a mild reaction condition efficiently and is recognized as the most promising removal method of organic sulfur.[9,10] The main hydrolysis reactions on the catalysts surfaces are listed as follow:

$$CS_2 + H_2O \rightarrow \mathrm{COS} + H_2S \quad (1)$$

$$COS + H_2O \rightarrow CO_2 + H_2S \quad (2)$$

$$H_2S + [O] \rightarrow H_2O + \mathrm{S}/SO_x^{2-} \quad (3)$$

$$S + [O] \rightarrow SO_x^{2-} \quad (4)$$

Organic COS or/and CS_2 are firstly adsorbed onto the -OH groups generated through the dissociation of H_2O via the ion-dipole interaction, and then gradually convert into the intermediate thiocarbonate ($HSCO_2^-$) under the action of -OH groups. Finally, $HSCO_2^-$ is further hydrolyzed into the easily removable H_2S.[11,12] Meanwhile, the formed H_2S can be adsorbed and oxidized to the deposited S or/and SO_4^{2-} by the oxygen-containing functional groups of catalyst which blocks the pore structure and occupies the active sites, resulting in the

poisoning/deactivation of the hydrolysis catalyst.[13] Furthermore, the presence of H_2O has a great influence on the hydrolysis performance of organic COS or/and CS_2. Yi et al. pointed out that the hydrolysis activity of catalyst was significantly low under the anhydrous atmosphere and the reintroduction of H_2O quickly improved the hydrolysis activity.[14] However, the presence of excess H_2O hindered the reaction between organic sulfur and active components of catalyst due to the formation of water film, and reduced the hydrolysis of COS or/and CS_2 because of the competitive adsorption of H_2O with organic sulfur on the catalysts surfaces.[15-17] Simultaneously, the enhancement of O_2 concentration during the hydrolysis process also made the hydrolysis activity of organic COS or/and CS_2 first increase and then decrease. The presence of low-concentration O_2 enhanced the oxidation of H_2S on the catalysts surfaces and promoted the catalytic hydrolysis of organic COS and CS_2, but the introduction of high-concentration O_2 led to a significant increase of H_2S oxidation and more sulfates were generated on the catalysts surfaces, which blocked the pore structure of catalyst and occupied the alkaline active sites, thereby decreased the hydrolysis activity of organic COS or/and CS_2.[13,18,19] However, the formation of surface sulfate species has been confirmed to improve the activity of cerium-based catalyst for selective catalytic reduction of NO_x with NH_3 (NH_3-SCR) due to the optimization of acid sites.[20,21]

At present, owing to the excellent oxygen storage capacity and significant redox properties, cerium-based catalyst has been regarded as a viable substitution for the traditional NH_3-SCR vanadium-based catalyst, but pure CeO_2 exhibited bad catalytic performance of NO_x reduction on account of poor surface acidity. Nevertheless, the sulfation treatment has been proposed to increase the acid sites and redox properties of CeO_2, and is a good strategy to optimize its NH_3-SCR activity by promoting the adsorption and activation of NH_3.[22-24] Yang et al. found that the gas-phase sulfation increased the adsorption capacity of NH_3 efficiently and enhanced the separation of -NH_2 adsorption sites and oxidation sites on CeO_2 surface, which inhibited the catalytic oxidation of -NH_2 to NO, improving the NH_3-SCR activity of CeO_2 catalyst.[25] Tan et al. had also mentioned that the gas phase sulfation led to the formation of more Ce^{3+}, oxygen vacancies and active acid sites on $Ce_{0.6}Zr_{0.4}O_2$ surface, and inhibited the formation of inactive nitrate.[26] These all contributed to enhancing the NH_3-SCR activity of cerium-based catalyst. Generally, as a typical component of the combustion flue gas of fossil fuel, SO_2 has widely been

used to optimize the NH_3-SCR activity of cerium oxide or/and cerium-based catalysts via the gas-phase sulfation, and the vulcanization conditions play an important role on regulating the sulfated degree of cubic fluorite CeO_2 and the formed types/amount of sulfate species in catalyst. Kwon et al. pointed out that the low-temperature gas-phase sulfation of SO_2 helped to the formation of surface sulfate species, but bulk sulfate species generated under the high-temperature gas-phase sulfation.[27] Furthermore, the enhancement of gas-phase sulfation time increased the formed amount of sulfate species on CeO_2 surface, which improved NH_3-SCR activity of catalyst significantly.[28] Interestingly, the anaerobic gas-phase sulfation of SO_2 had been found to further increase the concentrations of Ce^{3+} ions and oxygen vacancies on CeO_2 surface, which resulted in a significant enhancement in the NH_3-SCR performance and anti-SO_2 poisoning of catalyst.[29] However, compared to inorganic SO_2, organic CS_2/COS present stronger reducibility and our previous studies found that the gas-phase sulfation of reductive COS/CS_2 at 300 ^oC helped to induce more Ce^{3+}, active oxygen species and defects formed on the CeO_2 catalyst surface, thus exhibited better promotional effect on the NH_3-SCR activity than the traditional SO_2.[30] Furthermore, the NH_3-SCR activity of the sulfated CeO_2 catalyst has been found to be further increased when the gas-phase sulfation were carried out at the hydrolysis temperatures of organic COS or/and CS_2 (50 ^oC and 100 ^oC).

According to the above literatures about the catalytic hydrolysis of organic sulfur, the presence of H_2O/O_2 and their concentrations played an important role on the hydrolysis of organic COS/CS_2, which could regulate the formation of by-production sulfates in catalyst. Furthermore, it is noteworthy that the introduction of H_2O/O_2 might affect the NH_3-SCR activity of the sulfated CeO_2 catalyst during the low-temperature gas-phase sulfation of organic COS+CS_2. Because the formation of surface sulfate promoted the Brønsted acid sites of catalyst and contributed to the adsorption and activation of gaseous NH_3 over CeO_2. However, the formed bulk sulfate during the gas-phase sulfation hindered the redox performance and impeded the synergistic catalytic effect between surface sulfate and bulk CeO_2, thereby decreased the promotional effect of the gas-phase sulfation on the NH_3-SCR activity of CeO_2 catalyst.[31-33] Therefore, as the typical components of blast furnace gas, H_2O or/and O_2 were introduced into the gas-phase sulfation of organic COS+CS_2 at 50 ^oC in order to further improve the NH_3-SCR activity of the sulfated CeO_2-OS catalyst herein. The results confirm that the introduction of

appropriate H_2O or/and O_2 has a synergistic effect on increasing the NH_3-SCR performance of the sulfated CeO_2-OS catalyst by organic COS+CS_2 at 50 °C. Finally, some characterization techniques, including N_2 adsorption-desorption, Scanning electron microscopy (SEM), Transmission electron microscopy (TEM), high-resolution transmission electron microscopy (HR-TEM), X-ray diffraction (XRD), Raman spectroscopy (Raman), X-ray photoelectron spectroscopy (XPS), Temperature programmed reduction of H_2 (H_2-TPR), Temperature programmed desorption of NH_3 (NH_3-TPD) and Thermogravimetric (TG), were carried out to study the influence of H_2O or/and O_2 introduction on the physicochemical properties of CeO_2-OS catalyst. The results of this study are helpful to provide a new strategy for improving the NH_3-SCR activity of cerium oxide or/and cerium-based catalysts in the future.

2. Experimental

2.1. Catalyst preparation

Based on our previous researches, a one-pot hydrothermal method was used to synthesize CeO_2 catalyst with cerium nitrate ($Ce(NO_3)_3 \cdot 6H_2O$, AR), ammonium bicarbonate (NH_4HCO_3, AR) and hydrogen peroxide (30% H_2O_2, AR) as the precursor, precipitant and oxidant single CeO_2, respectively.[30,34]

The gas phase sulfation of CeO_2 was conducted in a tube furnace at 50 °C according to the hydrolysis temperature of organic sulfur.[3,15,19] The concentration and type of organic sulfur were chosen as follows: CS_2 30 ppm + COS 140 ppm (COS:CS_2=7:3 based on the number of sulfur atom in COS and CS_2), 0.33 vol.% H_2O (when used) and the concentrations of O_2 were selected as 0.3 vol.%, 5.0 vol.%, 10.0 vol.% (when applicable) according to the reported researches about the hydrolysis of COS or/and CS_2(Table S1). The total flow rate was set at 500 mL/min and N_2 (99.999 vol.%) was used to balance the mixture. The sulfation time for all samples was set at 3 hours. To simplify the identification, the pretreated catalysts were respectively labeled as CeO_2-OS, CeO_2-OS-O_2 (representing 5.0 vol.% O_2), CeO_2-OS-H_2O (representing 0.33 vol.% H_2O), and CeO_2-OS-O_2+H_2O, where OS denotes organic CS_2+COS. For example, CeO_2-OS-O_2+H_2O represents the gas-phase sulfated CeO_2-OS catalyst by organic CS_2+COS at 50 °C under the action of both 0.33 vol.% H_2O and 5.0 vol.% O_2. All samples were passed through a 40-60 mesh sieve for the activity evaluation.

2.2. Catalytic activity test

The NH_3-SCR catalytic performance was tested in a fixed bed micro-reactor at a temperature range of 150~400 °C by using 0.45 g catalyst. The corresponding gas hourly space velocity (GHSV) is 200,000 mL/(g·h) with the total flow rate of 1500 mL/min for the simulated flue gas. The simulated flue gas consists of 600 ppm NH_3, 600 ppm NO, 5.0 vol.% O_2 and balance gas 99.999 vol.% N_2. After the reaction system reaches a stable state, the activity test data is recorded to avoid the effect of gas adsorption over the catalyst. The concentrations of O_2 and NO_x at inlet and outlet were continuously monitored by T-350 flue gas analyzer (Testo, Germany), and the NO_x conversion rate (η) is calculated according to the following formula: $\eta = (1-[NO_x]_{out}/[NO_x]_{in})\times 100\%$, where $[NO_x]_{in}$ and $[NO_x]_{out}$ represent the inlet and outlet concentrations of gaseous NO_x (NO and NO_2), respectively.

2.3. Catalyst characterizations

The physical and chemical properties of catalysts were characterized by N_2 adsorption-desorption, scanning electron microscopy (SEM), transmission electron microscopy (TEM), high-resolution transmission electron microscopy (HR-TEM), X-ray diffraction (XRD), Raman spectroscopy (Raman), X-ray photoelectron spectroscopy (XPS), H_2 temperature programmed reduction (H_2-TPR), NH_3 temperature programmed desorption (NH_3-TPD) and thermogravimetric (TG) experiments.[30,35] The detailed test process is given in the Supplementary Information.

3. Results and discussion

3.1. Evaluation of catalytic activity

Our previous research found that the reductive organic sulfur presented better promotional effect on the NH_3-SCR activity of CeO_2 catalyst than the traditional SO_2 when the gas-phase sulfation was carried out at 300 ºC, and the promoting patterns of CS_2, COS and SO_2 were in according with their reducibility: CS_2 > COS > SO_2. Moreover, the introduction of 5.0 vol.% O_2 reduced the promotional effect of CS_2 on the catalytic activity, and CeO_2-CS_2+O_2-3h presented the similar NH_3-SCR activity to CeO_2-SO_2-3h.[30] Therefore, the influence of gas-phase sulfation temperature on the NH_3-SCR activity of the sulfated CeO_2 catalysts by organic COS or CS_2 was investigated, and the results are given in Fig. S1. It can be found that the decrease of the gas-

phase sulfation temperature from 300 ºC to 100 and 50 ºC contributes to enhancing the catalytic performance of the sulfated CeO_2 catalyst by organic CS_2. This phenomenon has also been confirmed for the gas-phase sulfation of COS (Fig.S1 (B)). At the same time, the hydrolysis conditions for organic COS/CS_2 have been summarized in Table S2. From Table S2, we can see that the hydrolysis of organic COS/CS_2 are usually carried out at the temperatures of 50~150 ºC. Therefore, in order to establish a connection between the NH_3-SCR activity and the hydrolysis of organic sulfur for CeO_2 catalyst, 50 ºC was chosen as the gas-phase sulfation temperature of COS+CS_2 to investigate the effect of components in blast furnace gas on the NH_3-SCR activity of the sulfated CeO_2-OS catalyst in the following sections.

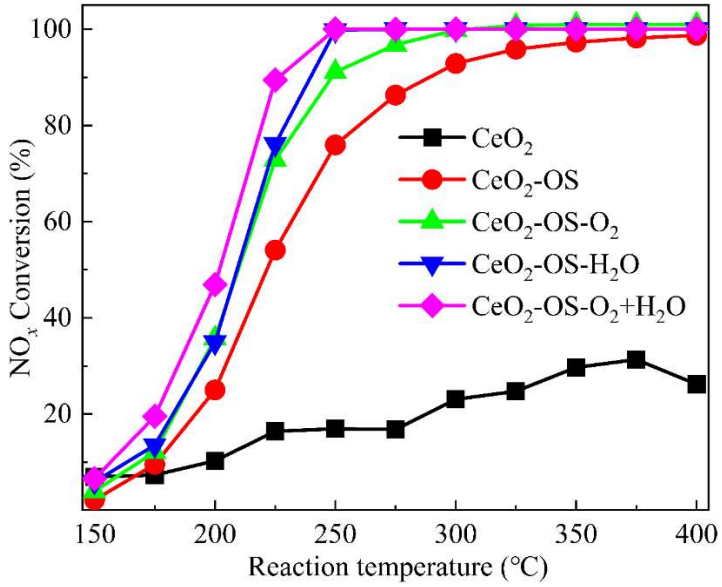

Fig. 1. Influence of H_2O or/and O_2 introduction on the NH_3-SCR activity of the gas-phase sulfated CeO_2 catalyst by organic CS_2+COS at 50 ºC for 3 h. The simulated flue gas components during the sulfation: CS_2 30 ppm + COS 140 ppm (COS:CS_2=7:3); H_2O=0.33 vol.% (when used); O_2=5.0 vol.% (when used).

As a typical component of blast furnace gas, the concentration of O_2 affected the formation of sulfates on the catalysts surfaces during the low-temperature hydrolysis of organic sulfur, and might affect the NH_3-SCR activity of the CeO_2 catalyst treated by the gas-phase sulfation of organic COS or/and CS_2. Therefore, it is very meaningfully to investigate the influence of O_2 introduced concentrations on the NH_3-SCR activity of the sulfated CeO_2-OS catalyst when the gas-phase sulfation is carried out at the low hydrolysis temperature of organic COS or/and CS_2. As shown in Fig. S2, the introduction of 0.3 vol.% O_2 scarcely affect the catalytic performance of CeO_2-OS catalyst, demonstrating that the presence of low concentration O_2 doesn't influence

197 the promotional effect of CS_2+COS gas-phase sulfation. However, the enhancement of O_2
198 concentration from 0.3 vol.% to 5.0 vol.% effectively enhances this promotional effect, which is
199 obviously different from the inhibition of 5.0 vol.% O_2 introduction on the NH_3-SCR activity of
200 the gas-phase sulfated CeO_2-OS catalyst by the reductive CS_2 at 300 °C, indicating that the
201 reducibility of COS or/and CS_2 might not influence the facilitation of their gas-phase sulfation at
202 the low hydrolysis temperature of organic sulfur on the NH_3-SCR activity of CeO_2 catalyst. But
203 the introduction of 5.0 vol.% O_2 might regulate the surface acid sites of the sulfated CeO_2-OS
204 catalyst by affecting the formation of sulfates. Instead, the further enhancement of O_2
205 concentration to 10.0 vol.% decreases the medium/high temperature NH_3-SCR activity of CeO_2-
206 OS catalyst. Therefore, the introduction of oxygen can affect the promotional effect of low-
207 temperature gas-phase sulfation of organic sulfur on the NH_3-SCR activity of the sulfated CeO_2-
208 OS catalyst, and the suitable introduced concentration of O_2 is 5.0 vol.%.

209 As another typical component of blast furnace gas, the presence of H_2O contributes to the
210 hydrolysis of organic sulfur on the basic catalysts surfaces which is an auxiliary agent for the
211 hydrolysis of COS or/and CS_2. Therefore, on the basis of the above research, water was also
212 introduced into the gas-phase sulfation of organic COS+CS_2 at 50 °C to investigate the influence
213 of H_2O introduction and its synergistic effect with oxygen, and the results are given in Fig. 1.
214 According to the results in Fig. 1, it can be found that introduction of 0.33 vol.% H_2O improves
215 the NH_3-SCR activity of the sulfated CeO_2-OS catalyst, and CeO_2-OS-H_2O presents better NO_x
216 reduction catalytic performance of 225-275 °C than CeO_2-OS-O_2. Furthermore, the introduction
217 of 5.0 vol.% O_2 further increases the low-temperature NH_3-SCR activity of CeO_2-OS-H_2O, and
218 there exists a certain synergistic promotional effect of O_2 and H_2O introduction on the catalytic
219 performance of NO_x reduction over the sulfated CeO_2-OS catalyst. Therefore, the CeO_2-OS-O_2,
220 CeO_2-OS-H_2O and CeO_2-OS-O_2+H_2O catalysts were chosen to be characterized in the following
221 sections to reveal the synergistic promotional effect of H_2O and O_2 introduction on the NH_3-SCR
222 activity of the gas-phase sulfated CeO_2-OS catalyst by organic COS+CS_2 at 50 °C.

223 **3.2. Morphological analysis**

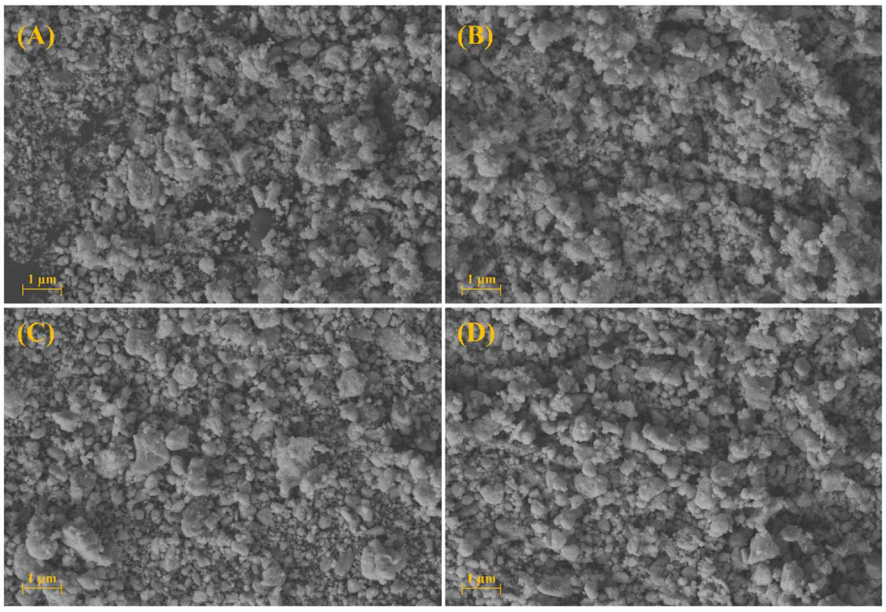

Fig. 2. The SEM images of (A) CeO_2-OS, (B) CeO_2-OS-O_2, (C) CeO_2-OS-H_2O and (D) CeO_2-OS-O_2+H_2O catalysts.

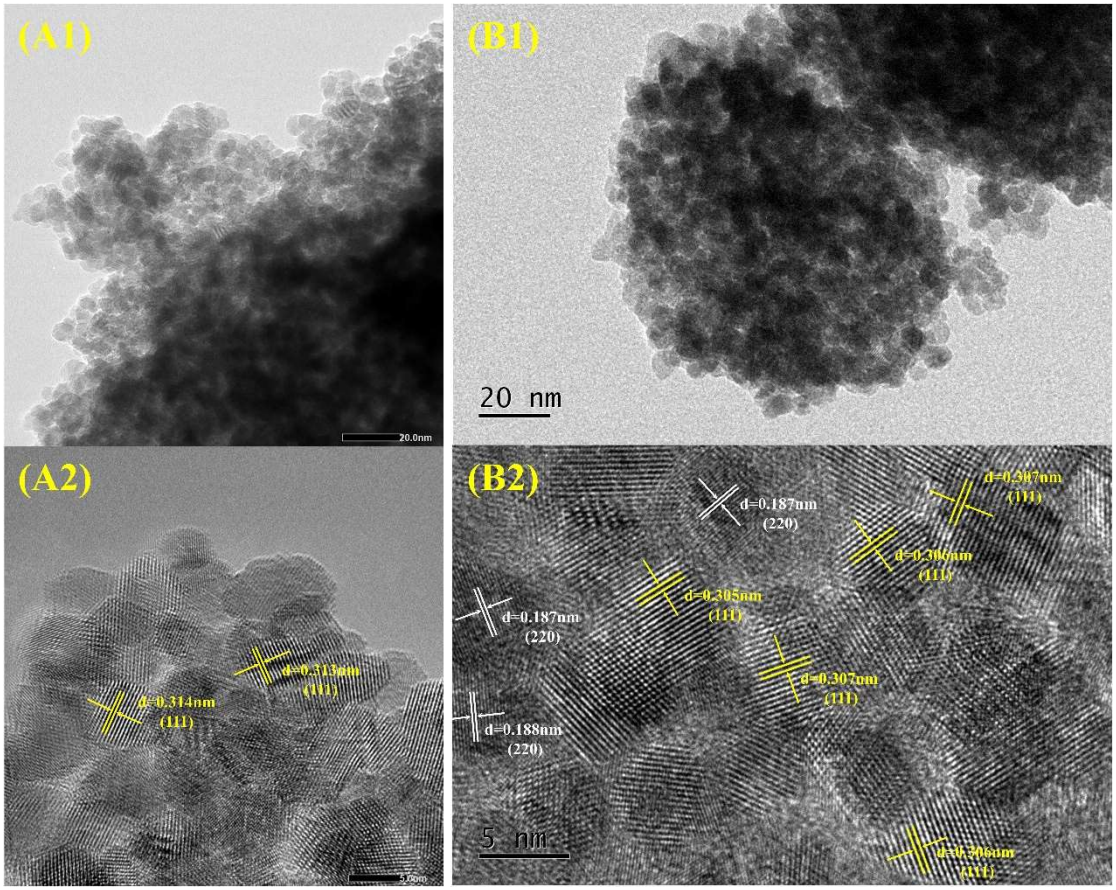

Fig. 3. The TEM/HR-TEM images of (A1)-(A2) CeO_2 and (B1)-(B2) CeO_2-OS-O_2+H_2O catalysts.

SEM and TEM/HR-TEM were obtained to investigate the influence of H_2O or/and O_2 introduction on the morphology of the gas-phase sulfated CeO_2-OS catalyst by organic

231 $COS+CS_2$ at 50 °C. According to the results of SEM in Fig. 2 and Fig. S3, it can be found that
232 the disorderly dispersed particles are presented on CeO_2-OS surface and there also exists a
233 certain degree of agglomeration for them due to the accumulation of nanoparticles. Meanwhile,
234 the introduction of O_2 or H_2O to the low-temperature gas-phase sulfation of organic $COS+CS_2$
235 slightly increases the agglomeration and crystallinity of nanoparticles on the surface of CeO_2-OS,
236 which is mainly attributed to the formation and deposition of sulfate species or/and sulfur
237 element on the catalyst surface, resulting in a decrease of specific surface area and pore volume.
238 Furthermore, the coexistence of O_2 and H_2O during the gas-phase sulfation of $COS+CS_2$ makes
239 the distribution of particles on the catalyst surface more uniform, which is conductive to the
240 formation of inter-particle pores.[36] Therefore, the TEM/HR-TEM images of CeO_2 and CeO_2-OS-
241 O_2+H_2O were also tested to study the influence of the low-temperature gas-phase sulfation of
242 organic $COS+CS_2$ at the presence of H_2O and O_2 on the structural morphology of CeO_2 catalyst.
243 As shown in Fig. 3, this gas-phase sulfation treatment makes the lattice spacing of 0.313 nm and
244 0.314 nm for the surface (111) crystal planes of cubic fluorite CeO_2 change to 0.305 nm, 0.306
245 nm and 0.307 nm owing to the lattice shrinkage caused by the deposition of sulfur element.[37]
246 Moreover, the deposition of sulfur element also leads to the appearance of the (220) crystal
247 planes with the lattice spacing of 0.187 nm and 0.188 nm.[38,39] The average diameters of nano-
248 particles on the CeO_2 and CeO_2-OS-O_2+H_2O surfaces were calculated according to the images of
249 TEM/HR-TEM. It can be found that the low-temperature gas-phase sulfation of organic
250 $COS+CS_2$ at the presence of H_2O and O_2 enhances the average particle diameters of cubic
251 fluorite CeO_2 from 4.78 nm to 4.93 nm, which might be attributed to the formation and
252 deposition of uniformly dispersed sulfates or/and sulfur element on the catalyst surface during
253 the low-temperature gas-phase sulfation of organic sulfur.

254 ## 3.3. Texture and structure characterization

255 In order to investigate the influence of H_2O or/and O_2 introduction on the pore structure of
256 the gas-phase sulfated CeO_2-OS catalyst by organic $COS+CS_2$ at 50 °C, the N_2 adsorption-
257 desorption characterization was carried out and the results are shown in Fig. 4 and Table 1.
258 According to IUPAC classification, the as-synthesized catalysts all exhibit the type IV isotherms
259 of N_2 adsorption-desorption and the related capillary-condensation hysteresis loop corresponds to
260 H3 type, which is usually attributed to the formed pores from the accumulation of

nanoparticles.[4,40] This is consistent with the results of SEM and TEM.

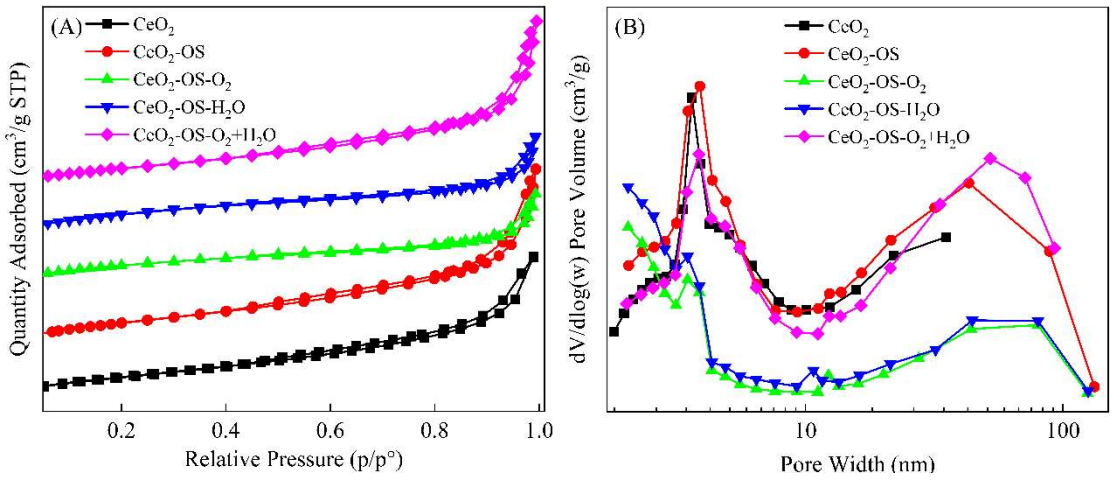

Fig. 4. The N_2 adsorption-desorption isotherms (A) and pore size distributions (B) of the as-synthesized catalysts.

Furthermore, the introduction of H_2O or O_2 during the gas-phase sulfation of organic COS+CS_2 makes the closing point of N_2 adsorption-desorption isotherm at low pressure for CeO_2-OS catalyst shift to right, indicating that the presence of H_2O or O_2 leads to the blocking of partial mesoporous and macro-porous pores of catalyst by regulating the formation and deposition of sulfates and sulfur element on cubic fluorite CeO_2 surface. Interestingly, CeO_2-OS-O_2+H_2O exhibits similar value of the closing point at low pressure to those of CeO_2-OS and CeO_2 catalysts, demonstrating that these three catalysts have similar pore size distributions and the co-existence of H_2O and O_2 during the gas-phase sulfation of organic COS+CS_2 overcomes their respective adverse effects on the blockage of the pore structure of CeO_2-OS catalyst to some extent. The results of pore size distribution in Fig. 4(B) indicate that the low-temperature gas-phase sulfation of organic COS+CS_2 presents almost no impact on the pore size distribution of CeO_2 catalyst, but the introduction of H_2O or O_2 during the gas-phase sulfation reduces the pore structure of CeO_2-OS catalyst at 2-100 nm. In addition, some microporous pores emerge for both CeO_2-OS-H_2O and CeO_2-OS-O_2 catalysts, and they present the distribution of the pore structure at both ends. However, the co-existence of H_2O and O_2 during the gas-phase sulfation eliminates this effect, and CeO_2-OS-O_2+H_2O also exhibits a bimodal pore size distribution as the same as those of CeO_2-OS and CeO_2 catalysts, although its mesoporous pores are less. The calculated results in Table 1 demonstrate that the introduction of H_2O or O_2 during the gas-phase sulfation reduces the BET surface area and pore volume of CeO_2-OS catalyst, despite CeO_2-OS-H_2O and CeO_2-OS-O_2 have smaller average pore sizes. According to the catalytic performance in

Fig. 1, the pore structure properties might not be the decisive factor for the NH_3-SCR activity of the gas-phase sulfated CeO_2-OS catalyst by organic COS+CS_2 under the conditions of H_2O or/and O_2.

Table 1 The physical structural parameters and the calculated oxygen vacancies of the as-prepared catalysts

Samples	BET surface area [a] (m^2/g)	Pore Volume [b] (cm^3/g)	Pore diameter [c] (nm)	$I_{(600+1180)}/I_{461}$ [d]
CeO_2	119.62	0.199	6.44	0.026
CeO_2-OS	127.86	0.280	8.34	0.032
CeO_2-OS-O_2	101.96	0.141	6.85	0.044
CeO_2-OS-H_2O	113.31	0.155	6.43	0.047
CeO_2-OS-O_2+H_2O	107.70	0.244	8.57	0.054

[a] BET surface area

[b] BJH desorption pore volume

[c] BJH desorption pore diameter

[d] Relative content of oxygen vacancies

The influence of H_2O or/and O_2 during the gas-phase sulfation on the X-ray diffraction (XRD) patterns of the sulfated CeO_2-OS catalyst by organic COS+CS_2 at 50 °C were measured, and the results are given in Fig. 5 and Fig. S5. According to the results of the X-ray diffraction (XRD) patterns, the as-synthesized CeO_2 catalyst has a typical cubic fluorite CeO_2 (PDF#34-0394) crystal according to the detected lattice diffraction peaks at 28.6°, 33.3°, 47.6°, 56.5°, 59.1°, 69.4°, 76.9° and 79.2°.[30] Meanwhile, the low-temperature gas-phase sulfation of organic COS+CS_2 effectively reduces the intensity of the lattice diffraction peaks attributed to cubic fluorite CeO_2 crystal for the as-synthesized CeO_2 catalyst. Interestingly, the introduction of H_2O or O_2 during the gas-phase sulfation decreases the sulfated degree of cubic fluorite CeO_2 crystal by organic COS+CS_2, and the CeO_2-OS-H_2O and CeO_2-OS-O_2 catalysts present stronger lattice diffraction peaks of cubic fluorite CeO_2 than CeO_2-OS. Furthermore, the co-introduction of H_2O and O_2 enhances this effect and CeO_2-OS-O_2+H_2O presents the strongest lattice diffraction peaks attributed to cubic fluorite CeO_2 among the gas-phase sulfated CeO_2-OS catalysts by organic COS+CS_2 at 50 °C. This indicates that the sulfation atmospheres absolutely affect the sulfated degree of cubic fluorite CeO_2 and thus regulate the formation and deposition of sulfur-containing

species in catalyst. The local XRD patterns at 15-30 ° in Fig. 5(B) confirm that the introduced H_2O or O_2 might play different roles on the formation of sulfur-containing species, and the introduction of O_2 helps to the crystallization of sulfates or/and sulfur element than H_2O in the sulfated CeO_2-OS catalyst. Previous researches had pointed out that the emerged diffraction peaks at 15-30 ° were mainly attributed to sulfate ($Ce_2(SO_4)_3 \cdot 4H_2O$ #38-0571, $Ce_2(SO_4)_3 \cdot 2H_2O$ #37-0762) and sulfur element (#34-0941) for the sulfated CeO_2 catalysts.[41,42] Hence, the existence of H_2O or/and O_2 can regulate the formation and deposition of sulfur-containing species in CeO_2 catalyst during the gas-phase sulfation of organic COS+CS_2 at 50 °C, and CeO_2-OS-O_2+H_2O exhibits similar lattice diffraction patterns of sulfates or/and sulfur element at 15~30 ° to CeO_2-OS-O_2.

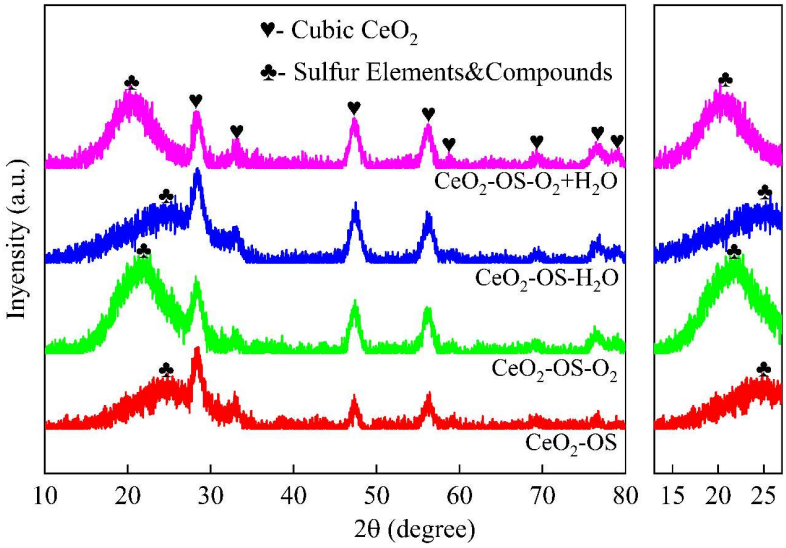

Fig. 5. The XRD patterns (A) and the locally XRD (10 ~ 30 °) (B) of the gas-phase sulfated CeO_2-OS catalysts.

The Raman spectra of CeO_2, CeO_2-OS, CeO_2-OS-O_2, CeO_2-OS-H_2O and CeO_2-OS-O_2+H_2O catalysts were tested to further investigate the formed sulfur-containing species on the structure of CeO_2 catalyst under the different atmospheres of low-temperature gas-phase sulfation. As shown in Fig. 6, it can be seen that three Raman characteristic peaks were detected for the as-synthesized catalysts. Among them, the band at 464 cm^{-1} is attributed to the F_{2g} vibrational mode of cubic fluorite ceria, which is viewed as the symmetric breathing of oxygen anions around cerium cations, while the bands at 600 cm^{-1} and 1180 cm^{-1} are ascribed to the characteristic peaks for the intrinsic oxygen vacancies from the reaction of $Ce^{4+} \rightarrow Ce^{3+}$.[26,43] Meanwhile, the low-temperature gas-phase sulfation of organic COS+CS_2 makes the F_{2g} vibration peak attributed to cubic fluorite CeO_2 shift from 464 cm^{-1} to 461 cm^{-1}, indicating the existence of the structural

change for the cubic fluorite CeO_2 under the interaction of the formed sulfur-containing species.[44] Furthermore, the introduction of H_2O exhibits stronger enhancement on the intensity of the F_{2g} vibration peak for the sulfated CeO_2-OS catalyst than O_2, and CeO_2-OS-O_2+H_2O presents similar intensity of this peak to CeO_2-OS-H_2O. Mei et al. pointed out that the red-shifted and increase of maximum half width values for the F_{2g} peaks resulted in the enhancement of oxygen vacancies, which was generally considered to facilitate the migration of oxygen atoms from the lattice position to the interstitial position, thus accelerated the conversion frequency between the chemisorbed oxygen and lattice oxygen on the catalysts surfaces.[45-47] Consequently, the relative concentrations of oxygen vacancies were quantified for the as-prepared catalysts by calculating "$I_{(600+1180)}/I_{461}$".[26,41] As shown in Table 1, the introduction of H_2O or/and O_2 during the gas-phase sulfation has a significant effect on the relative concentration of oxygen vacancies formed on the sulfated CeO_2-OS catalyst surface by organic COS+CS_2 at 50 °C and the calculated values decrease as follow: CeO_2-OS-O_2+H_2O > CeO_2-OS-H_2O > CeO_2-OS-O_2 > CeO_2-OS > CeO_2. Therefore, the co-existence of H_2O and O_2 presents a synergistic effect on enhancing the relative concentration of oxygen vacancies on the sulfated CeO_2-OS catalyst surface by improving the interaction between the formed sulfur containing species and the cubic fluorite CeO_2, and this pattern is consistent with the influence of H_2O or/and O_2 introduction on the NH_3-SCR activity of the sulfated CeO_2-OS catalyst by organic COS+CS2 at 50 °C.

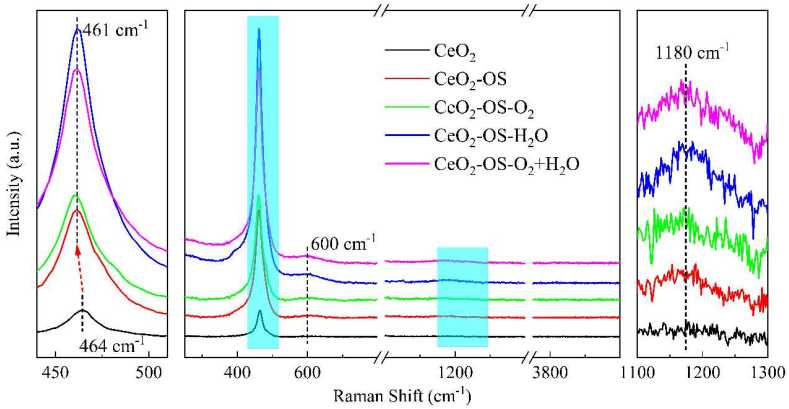

Fig. 6. The Raman spectra of CeO_2, CeO_2-OS, CeO_2-OS-O_2, CeO_2-OS-H_2O and CeO_2-OS-O_2+H_2O catalysts.

3.4. Surface active components analysis

The characterization results of N_2 adsorption-desorption, XRD and Raman all indicate that the introduction of H_2O or/and O_2 during the gas-phase sulfation affects the formation and

deposition of sulfur-containing species on the sulfated CeO_2-OS surface, thus influences the surface dispersion of elements and valences of catalyst, which have always been considered to be an important role on the NH_3-SCR activity. Hence, X-ray photoelectron spectroscopy (XPS) was tested to obtain the surface information of elements dispersion and valences over the as-synthesized catalysts. As shown in Fig 7(A), the Ce 3d spectra can be fitted into eight sub-peaks corresponding to four pairs of spin-orbit doublets, which are attributed to Ce^{4+} (u, u", u"', v, v" and v"') and Ce^{3+} (u' and v') species, respectively.[22,48] Meanwhile, the low-temperature gas-phase sulfation of organic COS+CS_2 makes the binding energies attributed to the Ce 3d XPS spectra of CeO_2 catalyst shift to left by reducing the electron cloud density around cerium ions via the interaction between the formed sulfate species and cubic fluorite CeO_2.[49,50] Zhang et al. pointed out that the doping of P element also led the binding energy of Ce 3d XPS spectra shift to higher value due to the electronic excitation effect of P and Ce ions on CeO_2 surface.[51] From Table 2, it can be found that the introduction of H_2O or O_2 during the gas-phase sulfation effectively improves the calculated molar ratio of $Ce^{3+}/(Ce^{3+}+Ce^{4+})$ on CeO_2-OS surface, although it decreases the formed quantity of sulfur-containing species. Furthermore, this promotional effect is further enhanced by the co-presence of H_2O and O_2, and CeO_2-OS-O_2+H_2O exhibits the largest surface molar ratio of $Ce^{3+}/(Ce^{3+}+Ce^{4+})$ and the least surface concentration of S element. Generally, the formation of Ce^{3+}/Ce^{4+} pairs contributes to the migration and release of lattice oxygen, thus higher surface $Ce^{3+}/(Ce^{3+}+Ce^{4+})$ molar ratio has usually been thought to be beneficial to the generation of surface oxygen vacancies and the NH_3-SCR activity of CeO_2 catalyst.[52,53] Therefore, the introduction of H_2O or/and O_2 during the gas-phase sulfation decreases the surface concentration of Ce species over the sulfated CeO_2 catalyst by organic COS+CS_2, but increases the molar ratio of $Ce^{3+}/(Ce^{3+}+Ce^{4+})$ on the catalyst surface, which might enrich the oxygen vacancies of catalyst. The results in Fig. 7(B) indicate that the O 1s spectra of CeO_2 can be fitted into three peaks located at about 529 eV, 530 eV and 531.8 eV, which are attributed to the lattice oxygen (O_α), the surface chemisorbed oxygen (O_β) and the lattice oxygen (O_γ) bonded with Ce_2O_3, respectively.[54,55] The gas-phase sulfation of organic COS+CS_2 decreases the total concentration of oxygen on CeO_2 surface, but improves the calculated surface $O_\beta/(O_\alpha+O_\beta+O_\gamma)$ molar ratio of catalyst, which is usually thought to promote the oxidation of NO to NO_2 and the NH_3-SCR activity via the “fast SCR” reaction.[56-58] Furthermore, the introduction

of H_2O or O_2 during the gas-phase sulfation further increases the molar ratio of $O_\beta/(O_\alpha+O_\beta+O_\gamma)$ on CeO_2-OS surface, and both CeO_2-OS-H_2O and CeO_2-OS-O_2 also present larger concentrations of total oxygen than that of CeO_2. In addition, there exist a synergistic promotional effect of H_2O and O_2 introduction on the formation of surface chemisorbed oxygen (O_β) of CeO_2-OS catalyst.

As shown in Fig. 7(C), the S 2p spectra of CeO_2-OS can be fitted into three sub-peaks located at 163.8 eV, 168.3 eV and 169.3 eV, and the first sub-peak is attributed to sulfur while the other two sub-peaks are ascribed to S^{6+} species.[59,60] Interestingly, the introduction of O_2 during the gas-phase sulfation leads the sub-peak of sulfur to disappear, indicating that the presence of O_2 promotes the oxidization of sulfur and the formation of sulfate species. Meanwhile, the sub-peak of sulfur still exists in CeO_2-OS-H_2O catalyst, but this peak also disappears after introducing oxygen together during the gas-phase sulfation. Thus, the sulfated atmosphere absolutely affects the conversion of the adsorbed COS+CS_2 on cubic fluorite CeO_2 surface, but the role of O_2 is obvious different from H_2O. The calculated data from XPS spectra in Table 2 indicate that the introduction of O_2 during the gas-phase sulfation enhances the surface sulfation of cubic fluorite CeO_2 and promotes the conversion of Ce^{4+} to Ce^{3+}, but it decreases the formation of sulfur-containing species on CeO_2-OS surface. This demonstrates that the presence of O_2 improves the formation of Ce^{3+}-based sulfates via enhancing the catalytic oxidization of sulfur, which increases the concentrations of total oxygen, $Ce^{3+}/(Ce^{3+}+Ce^{4+})$ and $O_\beta/(O_\alpha+O_\beta+O_\gamma)$ molar ratios on the catalyst surface. However, the introduction of H_2O also helps to the conversion of COS+CS_2 on cubic fluorite CeO_2 surface via its promotional effect on the hydrolysis of organic sulfur, and partial hydrolysis intermediate product of hydrogen sulfide desorbs from the surface of CeO_2.[18] As a consequence, less sulfur-containing species, including sulfates and sulfur, are formed on CeO_2-OS-H_2O surface, but this catalyst exhibits larger surface molar ratios of $Ce^{3+}/(Ce^{3+}+Ce^{4+})$ and $O_\beta/(O_\alpha+O_\beta+O_\gamma)$ than those of CeO_2-OS+O_2. Therefore, the co-existence of H_2O and O_2 presents a synergistic promotional effect on the conversion/hydrolysis of organic COS+CS_2 and the formation of dispersive sulfates on the surface of the low-temperature gas-phase sulfated CeO_2-OS catalyst. CeO_2-OS-O_2+H_2O has the largest surface $Ce^{3+}/(Ce^{3+}+Ce^{4+})$ and $O_\beta/(O_\alpha+O_\beta+O_\gamma)$ molar ratio, although its surface formed sulfur-containing species, mainly sulfates, is least compared to the CeO_2-OS, CeO_2-OS-O_2 and

CeO_2-OS-H_2O catalysts. Previous research confirmed that the formation of sulfate species improved the conversion of lattice oxygen to adsorbed oxygen on the catalysts surfaces during the gas-phase sulfation.[61,62] In addition, the presence of O_2 had been found to improve the oxidization of sulfur to SO_2 under the condition of sufficient oxygen content, and the present of low concentration H_2O promoted the hydrolysis activity of organic COS and CS_2 over catalyst, but high concentration H_2O led a film of water formed on the pore-structure of catalyst, which prevented the diffusing of organic COS and CS_2 to the hydrolytic active site, inhibiting the catalytic hydrolysis activity.[18,62,63] These all support the finding of this article about the influence of H_2O or/and O_2 introduction on the conversion and deposition of sulfur-containing species over the gas-phase sulfated CeO_2-OS catalyst by organic COS+CS_2 at 50 °C.

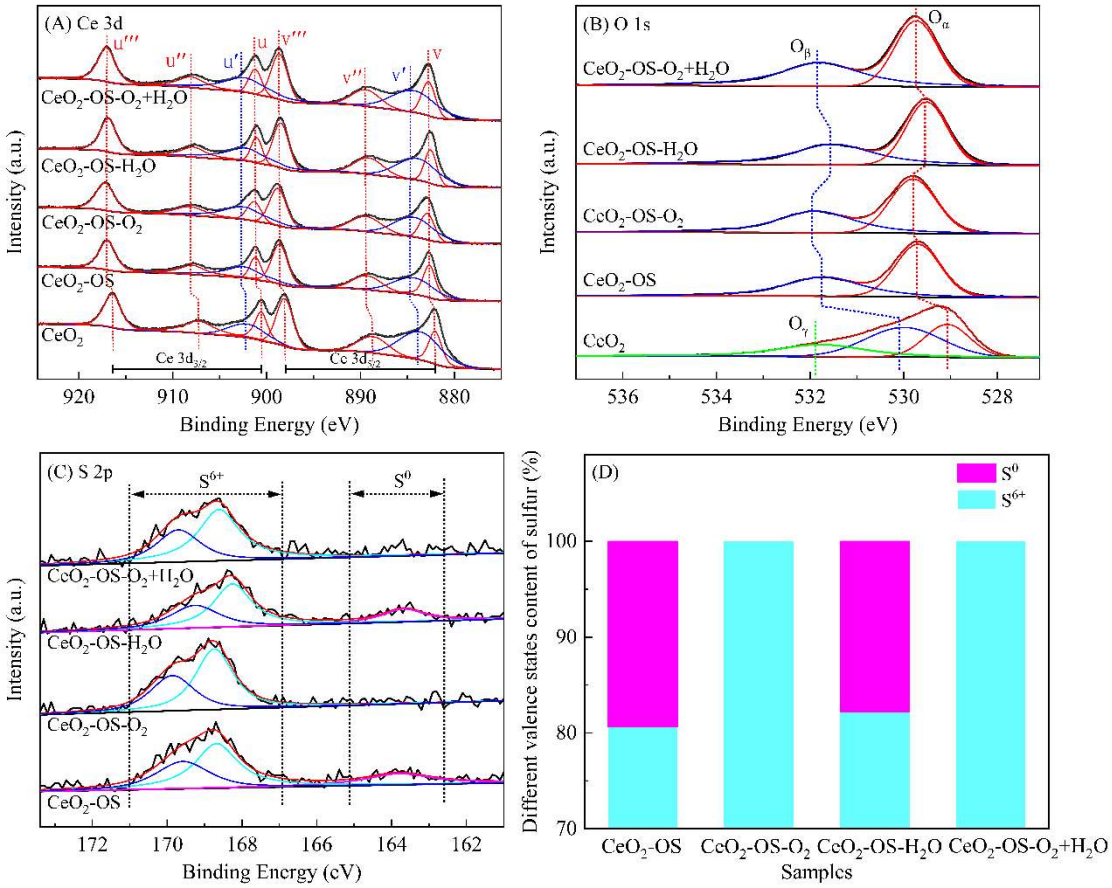

Fig. 7. The XPS spectra of CeO_2, CeO_2-OS, CeO_2-OS-O_2, CeO_2-OS-H_2O and CeO_2-OS-O_2+H_2O catalysts: (A) Ce 3d, (B) O 1s, (C) S 2p, (D) Sulfur valence distribution.

Table 2 The calculated surface compositions and atomic ratios of the as-prepared catalysts

Catalysts	Atomic concentrations (%)			Atomic ratios (%)	
	Ce	O	S[a]	$Ce^{3+}/(Ce^{3+}+Ce^{4+})$	$O_\beta/(O_\alpha+O_\beta+O_\gamma)$
CeO_2	36.16	63.84	-	31.34	44.16
CeO_2-OS	32.15	63.24	4.61	31.75	44.69
CeO_2-OS-O_2	30.92	65.30	3.78	36.08	46.32
CeO_2-OS-H_2O	32.73	63.94	3.33	36.42	46.79
CeO_2-OS-O_2+H_2O	31.63	65.18	3.19	37.57	48.54

[a] the sum of S^{6+} and S^0 calculated from the XPS spectra.

3.5. Thermogravimetric analysis

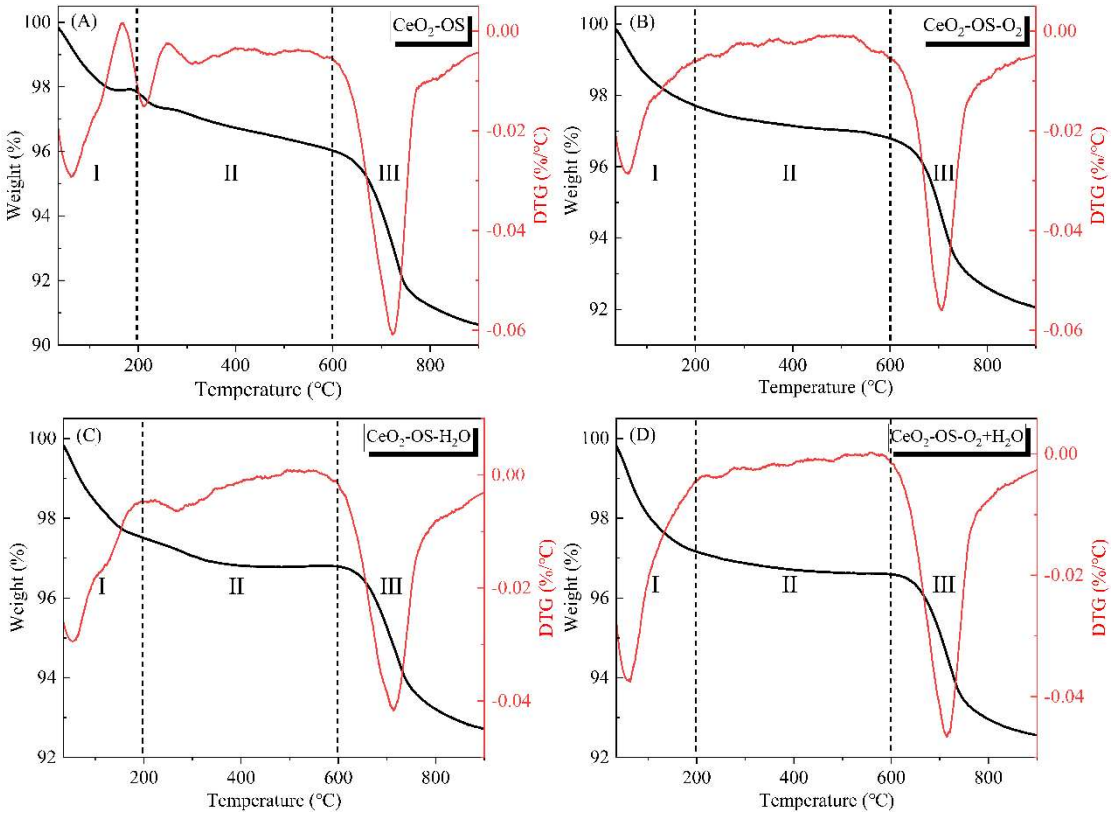

Fig. 8. The TG-DTG curves of CeO_2-OS, CeO_2-OS-O_2, CeO_2-OS-H_2O and CeO_2-OS-O_2+H_2O catalysts.

The results of XPS spectra indicate that the introduction of H_2O or/and O_2 during the gas-phase sulfation can regulate the formation of sulfur-containing species, including sulfates and sulfur, on the gas-phase sulfated CeO_2-OS catalyst by organic COS+CS_2 at 50 °C. Hence, the thermal characteristics of conversion and decomposition for the formed sulfur-containing species

were studied by thermogravimetric analysis in order to further investigate the influence of H_2O or/and O_2 introduction, and the results are shown in Fig. 8. The thermal weight loss of the sulfated CeO_2-OS catalyst can be divided into three parts, and the steep weight loss peak observed at 30-200 °C is mainly attributed to the desorption of the physically absorbed water or/and the de-hydroxylation.[24] In addition, the slight weight loss observed at 200-600 °C is ascribed to the emission of SO_2 via the oxidization of the formed sulfur in the CeO_2-OS catalyst by its inherent oxygen-containing functional groups. Finally, the third weight loss detected at 600-800 °C is attributed to the decomposition of sulfates formed in catalyst.[23,31] However, the introduction of O_2 during the gas-phase sulfation makes the second weight loss ascribed to the oxidization of sulfur almost disappear, indicating that the presence of O_2 restricts the formation of sulfur in the CeO_2-OS+O_2 catalyst via the oxidation reaction, which is in accordance with the results of XPS spectra in Section 3.4, although XPS is a surface-sensitive technique that mainly detects the elemental composition on the catalysts surfaces.[17,64] Furthermore, the third weight loss attributed to the decomposition of sulfates also decreases under the condition of O_2, demonstrating that the introduction of O_2 during the gas-phase sulfation promotes the desorption of the sulfur-containing intermediates rather than the further oxidation to sulfates. Interestingly, the introduction of 0.33 vol.% H_2O exhibits better promotional effect on reducing the formed quality of sulfates than 5.0 vol.% O_2, which might be attributed to its improved effect on the conversion of organic COS+CS_2 on cubic fluorite CeO_2 surface by optimizing the hydrolysis activity. It should be mentioned that the calculated mass of the second weight loss attributed to the oxidization of sulfur to SO_2 decreases as follow for the sulfated CeO_2 catalysts: CeO_2-OS (0.91%) > CeO_2-OS-H_2O (0.47%) > CeO_2-OS-O_2 (0.37%) > CeO_2-OS-O_2+H_2O (0.29%). This indicates that the presence of O_2 exhibits better promotional effect on restricting the formation of sulfur during the low-temperature gas-phase sulfation of organic COS+CS_2 than H_2O, and the co-introduction of O_2 further decreases the formed quality of sulfur in the CeO_2-OS-H_2O catalyst. There exists a synergistic effect of H_2O and O_2 introduction on reducing the formed amount of sulfur and sulfates during the low-temperature gas-phase sulfated CeO_2-OS catalyst by organic COS+CS_2. As shown in Fig. 1, Fig. 7, Fig. 8 and Table 3, CeO_2-OS-O_2+H_2O has the least sulfur-containing species compared to the other sulfated catalysts, but presents the best NH_3-SCR activity. This demonstrates that the formed highly dispersive sulfates might play an important

role on influencing the catalytic performance of NO_x reduction over the low-temperature gas-phase sulfated CeO_2-OS catalyst by COS+CS_2 at the presence of H_2O or/and O_2.

Table 3. The results of mass loss of sulfate and the calculated peak areas of the H_2-TPR spectra for the as-prepared catalysts

Samples	Mass loss of sulfate [a] (%)	H_2-TPR peak area (a.u.)		
		I	II	III
CeO_2	-	922	-	1274
CeO_2-OS	5.44	462	6550	1956
CeO_2-OS-O_2	4.74	877	4905	903
CeO_2-OS-H_2O	4.07	672	5939	2066
CeO_2-OS-O_2+H_2O	4.05	876	5418	1895

[a] the mass loss of sulfate calculated from the TG-DTG curves.

3.6. The properties of redox ability and surface acidity

The redox properties and acid sites have been usually thought to play an important role on the NH_3-SCR activity of catalyst.[65,66] Hence, H_2-TPR and NH_3-TPD were also carried out to investigate the influence of H_2O or/and O_2 introduction during the gas-phase sulfation on the redox properties and acid sites of the sulfated CeO_2-OS catalyst by organic COS+CS_2 at 50 °C. According to the results of H_2-TPR in Fig. 9 and Table. 3, it can be seen that two broad reduction peaks at 400~550 °C (region I) and 700~900 °C (region III) are detected for CeO_2, which are attributed to the reduction of Ce^{4+} to Ce^{3+} on the surface and sub-surface of CeO_2 and the reduction of Ce^{4+} to Ce^{3+} in the bulk phase, respectively. In addition, one new reduction peak ascribed to the formed metal sulfate species appears at 500~700 °C (region II) for the sulfated CeO_2-OS catalysts.[67,68] In region I, the introduction of H_2O or/and O_2 during the low-temperature gas-phase sulfation of organic COS+CS_2 makes the reduction temperature shift toward lower temperature and increases the amount of reduced species, which might be attributed to the fact that the adsorbed organic COS+CS_2 reacts with the oxygen-containing functional groups on cubic fluorite CeO_2 surface, bringing the sulfated-induced degradation of the Ce-O bond in catalyst and promoting an increase in surface Ce^{3+} and oxygen vacancies.[30,69] In addition, the temperatures of the reduction peaks for the CeO_2-OS-O_2, CeO_2-OS-O_2+H_2O catalysts within

region II and III are lower than that of CeO_2-OS. This indicates that the introduction of O_2 or/and H_2O into the simulated gas-phase sulfation atmosphere leads the metal sulfate formed on the catalysts surfaces to be reduced easier.[70] Moreover, CeO_2-OS-O_2+H_2O has more reduction species than CeO_2-OS-O_2 catalyst, which might be an important reason for its good NH_3-SCR activity. Therefore, the introduction of O_2 or/and H_2O into the gas-phase sulfation atmosphere of organic COS+CS_2 at 50 °C modulates the reducibility of the sulfated CeO_2-OS catalyst by affecting the conversion of the surface adsorbed COS+CS_2 into the reducible metal sulfates.

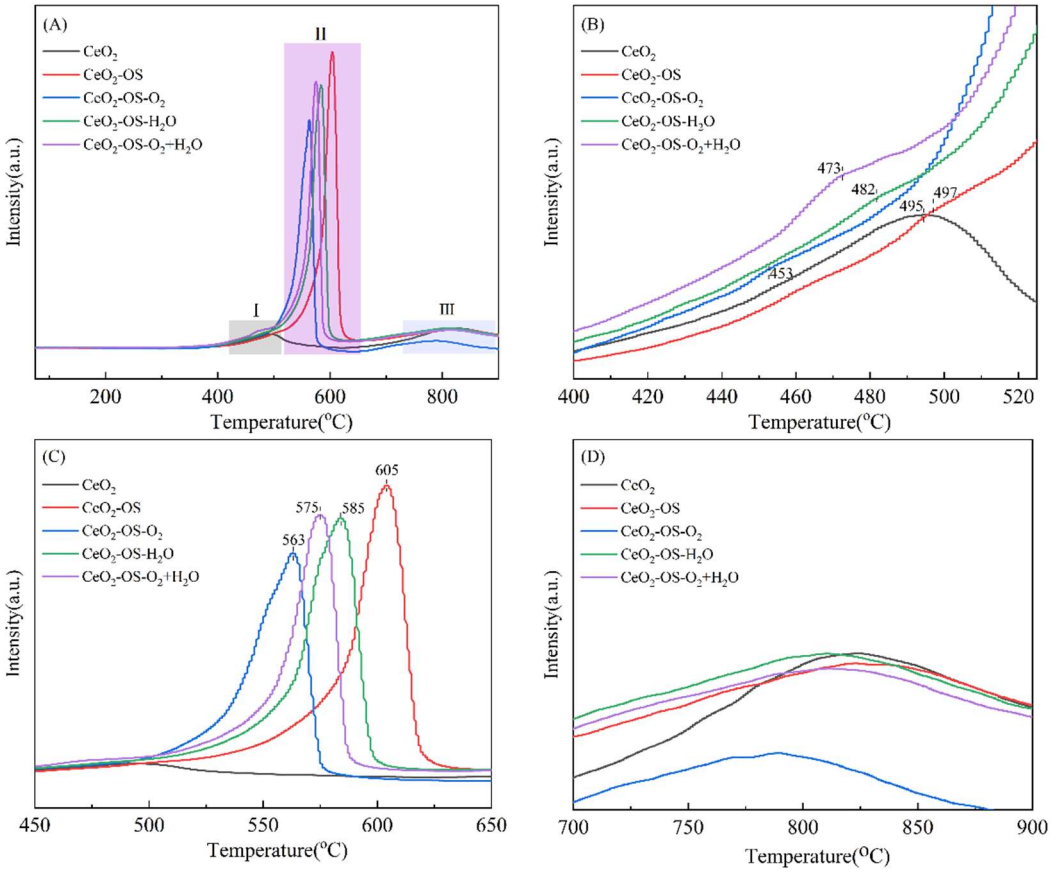

Fig. 9. The H_2-TPR profiles of CeO_2, CeO_2-OS, CeO_2-OS-O_2, CeO_2-OS-H_2O and CeO_2-OS-O_2+H_2O catalysts.

Our previous study had confirmed that the gas-phase sulfation of reductive organic CS_2 at 300 °C induced more SO_4^{2-} formed in cerium oxide and improved the surface acid sites of catalyst, especially the low-temperature Lewis acid sites, thus presented better promotional effect on the NH_3-SCR activity of CeO_2 catalyst than the traditional inorganic SO_2.[30] Furthermore, the NH_3 desorption peak at lower temperature was attributed to the weak acid sites and physically adsorbed NH_3 species, and the desorption peak at higher temperature was ascribed to the NH_3 species adsorbed on the medium-strong acid sites.[58,71,72] Based on the NH_3-TPD spectra of the

gas-phase sulfated CeO_2-OS catalysts, it can be found that the introduction of H_2O or O_2 decreases the weak acid sites of CeO_2-OS catalyst, and the co-existence of H_2O and O_2 further enhances this reduction, indicating that the introduction of H_2O or/and O_2 during the gas-phase sulfation is unbeneficial to the formation of weak acid sites for the sulfated CeO_2-OS catalyst by organic COS+CS_2 at 50 °C because of their effect on reducing the formed quality of sulfates. It should be mentioned that the introduction of H_2O or/and O_2 during the gas-phase sulfation makes the peak position of the weak acid sites for the CeO_2-OS catalyst shift to lower temperature. This demonstrates that the adsorbed NH_3 species over the weak acid sites are easily desorbed from the surface of CeO_2-OS-O_2, CeO_2-OS-H_2O and CeO_2-OS-O_2+H_2O catalysts, and present higher reactivity for NH_3-SCR. Furthermore, the co-existence of H_2O and O_2 also improves the medium-strong acid sites of CeO_2-OS catalyst although CeO_2-OS-O_2+H_2O has the least formed sulfates compared to the other sulfated CeO_2-OS catalyst. The calculated molar ratio of medium-strong acid sites and weak acid sites in Fig. 10(B) confirms that the introduction of H_2O or/and O_2 during the gas-phase sulfation all increase the proportion of medium-strong acid sites for the sulfated CeO_2-OS catalyst, and the calculated values decrease as follow: CeO_2-OS-O_2+H_2O (35.1%) > CeO_2-OS-H_2O (24.1%) > CeO_2-OS-O_2 (23.7%) > CeO_2-OS (21.4%), which is in accordance with the NH_3-SCR activity. Previous studies pointed out that the formation of medium-strong acid sites contributed to inhibiting the excessive oxidation of NH_3 on the catalysts surfaces, thereby inhibited the non-selective catalytic oxidation of NH_3 and increased the utilization coefficient of NH_3.[24] Therefore, it can be induced that the introduction of H_2O or/and O_2 during the gas-phase sulfation decreases the formed quality of sulfur-containing species, including sulfur and sulfates, in the sulfated CeO_2-OS catalysts by organic COS+CS_2 at 50 °C, but the less and highly dispersive sulfates are beneficial to activate the adsorbed NH_3 species over the weak acid sites of catalyst and also improve the proportion of medium-strong acid sites, especially the co-existence of H_2O and O_2. This might be one of the important reasons for the excellent NH_3-SCR activity of the CeO_2-OS-O_2+H_2O catalyst.

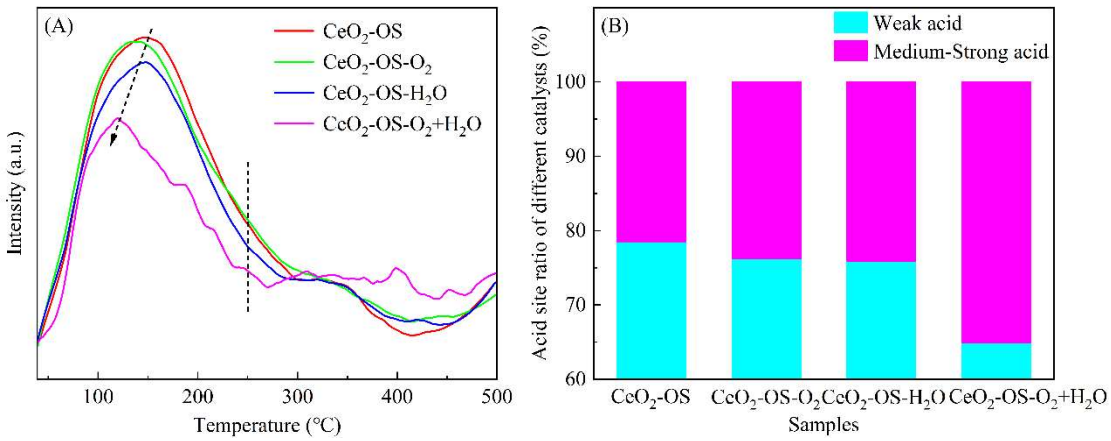

Fig. 10. The NH_3-TPD profiles of the gas-phase sulfated CeO_2-OS catalysts by organic CS_2+COS.

4. Conclusions

As the typical components of blast furnace gas, H_2O or/and O_2 were introduced during the low-temperature gas-phase sulfation to improve the NH_3-SCR activity of the sulfated CeO_2-OS catalyst by organic COS+CS_2, and there exists a synergistic promotional effect of H_2O and O_2 introduction on the catalytic performance of NO_x reduction over CeO_2-OS. The characterization results demonstrate that the introduction of 5.0 vol.% O_2 or 0.33 vol.% H_2O during the gas-phase sulfation enhances the conversion of organic COS+CS_2 on cubic fluorite CeO_2 surface, which reduces the formation of sulfur-containing species in catalyst, including sulfur and sulfates, and decreases the BET surface area and pore volume of CeO_2-OS. However, the introduction of O_2 or H_2O during the gas-phase sulfation effectively increases the molar ratio of $Ce^{3+}/(Ce^{3+}+Ce^{4+})$ and $O_\beta/(O_\alpha+O_\beta+O_\gamma)$ on CeO_2-OS surface, thus more oxygen vacancies and chemisorbed oxygen are generated. These properties of catalyst are further enhanced by the co-existence of O_2 and H_2O during the gas-phase sulfation. Furthermore, the reduction of the formed sulfates under the action of introduced O_2 or H_2O decreases the weak acid sites of CeO_2-OS catalyst, but the less and highly dispersive sulfates presents stronger reducibility. However, the introduction of H_2O or/and O_2 during the gas-phase sulfation increases the proportion of medium-strong acid sites for CeO_2-OS catalyst. These all might be the important reasons for the promotional effect of H_2O or/and O_2 introduction on the NH_3-SCR activity. Therefore, there exists a synergistic effect of H_2O and O_2 introduction during the gas-phase sulfation on the physical-chemical properties and catalytic performance of the sulfated CeO_2-OS catalyst by organic COS+CS_2 at 50 °C.

CRediT authorship contribution statement

Zhibo Xiong: Conceptualization, Funding acquisition, Writing - review & editing. **Yafei Zhu and Jiaxing Liu:** Writing - original draft, Methodology, Validation. **Yanping Du:** Writing - review & editing. **Fei Zhou:** Investigation, Supervision. **Jing Jin and Qiguo Yang:** Investigation, Supervision, Writing - review & editing. **Wei Lu:** Investigation, Supervision.

Declaration of Competing Interest

The authors declare that they have no known competing financial interests or personal relationships that could have appeared to influence the work reported in this paper.

Acknowledgements

This work was supported by the National Science Foundation of China (No. 51406118), the Bureau of Shanghai Municipal Science and Technology (No. 23010503500).

References

[1] X. An, L. H. Zhu, J. Xiao, W. Jiang, X. Gao, L. X. Xu, H. P. Li, W. S. Zhu and H. M. Li, Engineering hollow mesoporous silica supported cobalt molybdate catalyst by dissolution-regrowth strategy for efficiently aerobic oxidative desulfurization, Fuel, 2022, 325, 124755.

[2] P. Xu, Z. H. Jin, T. Y. Zhang, X. F. Chen, M. H. Qiu and Y. Q. Fan, Fabrication of a Ceramic Membrane with Antifouling PTFE Coating for Gas-Absorption Desulfurization, Ind. Eng. Chem. Res., 2021, 60, 2492-2500.

[3] R. X. Xiao, K. F. Chao, J. Liu, M. H. Chen, X. B. Zhu and B. Fu, Screening of Absorbents for Viscose Fiber CS_2 Waste Air and Absorption–Desorption Process, Atmosphere, 2023, 14, 602.

[4] J. Arfaoui, A. Ghorbel, C. Petitto and G. Delahay, Effect of acidic components (SO_4^{2-} and WO_3) on the surface acidity, redox ability and NH_3-SCR activity of new CeO_2-TiO_2 nanoporous aerogel catalysts: A comparative study, Inorg. Chem. Commun., 2022, 140, 109494.

[5] F. Minichilli, F. Gorini, E. Bustaffa, L. Cori and F. Bianchi, Mortality and hospitalization associated to emissions of a coal power plant: A population-based cohort study, Sci. Total Environ., 2019, 694, 133757.

[6] S. M. Wang, Near-Zero Air Pollutant Emission Technologies and Applications for Clean Coal-Fired Power, Engineering, 2020, 6, 1408-1422.

[7] H. Y. Wang, H. H. Yi, P. Ning, X. L. Tang, L. L. Yu, D. He and S. Z. Zhao, Calcined hydrotalcite-like compounds as catalysts for hydrolysis carbonyl sulfide at low temperature, Chem. Eng. J., 2011, 166, 99-104.

[8] L. C. Seefeldt, M. E. Rasche and S. A. Ensign, Carbonyl Sulfide and Carbon Dioxide as New Substrates, and Carbon Disulfide as a New Inhibitor, of Nitrogenase, Biochemistry, 1995, 34, 5382-5389.

[9] J. X. Mi, G. Q. Zhang, Q. Y. Zhang, W. T. Zhao, Y. N. Cao, F. J. Liu and L. L. Jiang, Defects modulating on MgAl-hydrotalcite nanosheet with improved performance in carbonyl sulfide elimination via a hydroxyl chemical looping route, Chem. Eng. Sci., 2022, 259, 117827.

[10] K. L. Li, G. Liu, C. Wang, K. Li, X. Sun, X. Song and P. Ning, Acidic and basic groups introducing on the surface of activated carbon during the plasma-surface modification for changing of COS catalytic hydrolysis activity, Catal. Commun., 2020, 144, 106093.

[11] S. Han, H. Yang, P. Ning, K. Li, L. H. Tang, C. Wang, X. Sun and X. Song, Density functional theory study on the hydrolysis process of COS and CS_2 on a graphene surface, Res. Chem. Intermed., 2018, 44, 2637-2651.

[12] N. Liu, X. Song, C. Wang, K. Li, P. Ning, X. Sun, F. Wang and Y. X. Ma, Surface characterization study of corn-straw biochar catalysts for the simultaneous removal of HCN, COS, and CS_2, New J. Chem., 2020, 44, 13565.

[13] L. Wang, S. D. Wang, Q. Yuan and G. Z. Lu, COS hydrolysis in the presence of oxygen: Experiment and modeling, J. Nat. Gas Chem., 2008, 17, 93-97.

[14] H. H. Yi, C. C. Du, X. D. Zhang, S. Z. Zhao, X. Z. Xie, L. L. Miao and X. L. Tang, Inhibition of CO in Blast Furnace Flue Gas on Poisoning and Deactivation of a Ni/Activated Carbon Catalyst in COS Hydrolysis, Ind. Eng. Chem. Res., 2021, 60, 18183-18193.

[15] H. H. Han, Z. H. Zhang and Y. L. Zhang, Research on the Catalytic Hydrolysis of COS by Fe-Cu/AC Catalyst and Its Inactivation Mechanism at Low Temperature, Energy Technology & Environmental Science, 2022, DOI:10.1002/slct.202200194.

[16] Z. Sun, J. P. Liu and Z. Q. Sun, Synergistic decarbonization and desulfurization of blast furnace gas via a novel magnesium-molybdenum looping process, Fuel, 2020, 279, 118418.

[17] R. H. Sui, C. B. Lavery, C. E. Deering, R. Prinsloo, D. Li, N. Chou, K. L. Lesage and R. A. Marriott, Improved carbon disulfide conversion: Modification of an alumina Claus catalyst by deposition of transition metal oxides, Appl. Catal. A-Gen., 2020, 604, 117773.

[18] X. Sun, H. T. Ruan, X. Song, L. N. Sun, K. Li, P. Ning and C. Wang, Research into the reaction process and the effect of reaction conditions on the simultaneous removal of H_2S, COS and CS_2 at low temperature, RSC Adv., 2018, 8, 6996.

[19] J. N. Gu, J. X. Liang, S. J. Hu, Y. X. Xue, X. Min, M. M. Guo, X. F. Hu, J. P. Jia and T. H. Sun, Enhanced removal of COS from blast furnace gas via catalytic hydrolysis over Al_2O_3-based catalysts: Insight into the role of alkali metal hydroxide, Sep. Purif. Technol., 2022, 295 121356.

[20] Z. W. Gu, L. J. Cheng, C. Tan, S. Sin, C. K. Huang and C. J. Tang, Enriching SO_4^{2-} Immobilization on α-Fe_2O_3 via Spatial Confinement for Robust NH_3-SCR Denitration, Catalysts, 2022, 12, 991.

[21] M. Y. Guo, Q. L. Liu, P. P. Zhao, J. F. Han, X. Li, Y. Ha, Z. C. Fu, C. F. Song, N. Ji, C. X. Liu, D. G. Ma and Z. G. Li, Promotional effect of SO_2 on Cr_2O_3 catalysts for the marine NH_3-SCR reaction, Chem. Eng. J., 2019, 361, 830-838.

[22] S. H. Wang, C. Fan, Z. Q. Zhao, Q. Liu, G. Xu, M. H. Wu, J. J. Chen and J. H. Li, A facile and controllable in situ sulfation strategy for CuCeZr catalyst for NH_3-SCR, Appl. Catal. A-Gen., 2020, 597, 117554.

[23] Z. X. Song, Q. L. Zhang, P. Ning, X. Liu, J. Fan and Z. Z. Huang, Introduction manner of sulfate acid for improving the performance of SO_4^{2-}/CeO_2 on selective catalytic reduction of NO by NH_3, J. Rare Earths, 2016, 34, 667.

[24] Q. L. Zhang, J. H. Zhang, Z. X. Song, P. Ning, H. Li and X. Li, A novel and environmentally friendly SO_4^{2-}/CeO_2 catalyst for the selective catalytic reduction of NO with NH_3, J. Ind. Eng. Chem., 2016, 34, 165-171.

[25] S. J. Yang, Y. F. Guo, H. Z. Chang, L. Ma, Y. Peng, Z. Qu, N. Q. Yan, C. Z. Wang and J. H. Li, Novel effect of SO_2 on the SCR reaction over CeO_2: Mechanism and significance, Appl. Catal., B, 2013, 136-137, 19-28.

[26] W. Tan, J. M. Wang, L. L. Li, A. N. Liu, G. Song, K. Guo, Y. D. Luo, F. D. Liu, F. Gao and L. Dong, Gas phase sulfation of ceria-zirconia solid solutions for generating highly efficient and SO_2 resistant NH_3-SCR catalysts for NO removal, J. Hazard. Mater., 2020, 388, 121729.

[27] D. W. Kwon, J. Kim and H. P. Ha, Establishment of surface/bulk-like species functionalization by controlling the sulfation temperature of Sb/V/Ce/Ti for NH_3-SCR, Appl. Surf. Sci., 2019, 481, 1503-1514.

[28] Q. Xie, Y. D. Cai, L. Zhang, Z. H. Hu, T. Z. Li, X. D. Wang, Q. Zeng, X. Wang, J. F. Sun and L. Dong, Relationships between Adsorption Amount of Surface Sulfate and NH_3-SCR Performance over CeO_2, J. Phys. Chem. C, 2021, 125, 21964-21974.

[29] J. J. Chen, W. T. Zhao, Q. Wu, J. X. Mi, X. Y. Wang, L. Ma, L. L. Jiang, C. T. Au and J. H. Li, Effects of anaerobic SO_2 treatment on nano-CeO_2 of different morphologies for selective catalytic reduction of NO_x with NH_3, Chem. Eng. J., 2020, 382, 122910.

[30] W. Wang, Z. B. Xiong, J. Jin, W. Lu and H. C. Shi, Influence of CS_2 pretreatment on the NH_3-SCR activity

of CeO_2: Synergistic promotional effect of sulfation and reduction, J. Environ. Chem. Eng., 2021, 9, 106836.

[31] L. Zhang, L. L. Li, Y. Cao, X. J. Yao, C. Y. Ge, F. Gao, Y. Deng, C. J. Tang and L. Dong, Getting insight into the influence of SO_2 on TiO_2/CeO_2 for the selective catalytic reduction of NO by NH_3, Appl. Catal., B, 2015, 165, 589-598.

[32] W. Tan, J. M. Wang, S. H. Yu, A. N. Liu, L. L. Li, K. Guo, Y. D. Luo, S. H. Xie, F. Gao, F. D. Liu and L. Dong, Morphology-Sensitive Sulfation Effect on Ceria Catalysts for NH_3-SCR, Top. Catal., 2020, 63, 932-943.

[33] H. Z. Chang, L. Ma, S. J. Yang, J. H. Li, L. Chen, W. Wang and J. M. Hao, Comparison of preparation methods for ceria catalyst and the effect of surface and bulk sulfates on its activity toward NH_3-SCR, J. Hazard. Mater., 2013, 262, 782-788.

[34] W. Wang, Z. B. Xiong, W. F. He, W. Lu and H. C. Shi, Influence of thiourea modification on the NH_3-SCR activity of CeO_2: Simultaneous tuning morphology and surface acidity, J. Energy Inst., 2021, 98, 322-333.

[35] C. X. Li, Z. B. Xiong, J. F. He, X. K. Qu, Z. Z. Li, X. Ning, W. Lu, S. M. Wu and L. Z. Tan, Influence of ignition atmosphere on the structural properties of magnetic iron oxides synthesized via solution combustion and the NH_3-SCR activity of W/Fe_2O_3 catalyst, Appl. Catal. A-Gen., 2020, 602, 117726.

[36] Y. Y. Dong, B. F. Jin, S. M. Liu, J. J. Gao, K. J. Wang and F. B. Su, Abundant Oxygen Vacancies Induced by the Mechanochemical Process Boost the Low-Temperature Catalytic Performance of MnO_2 in NH_3-SCR, Catalysts, 2022, 12 1291.

[37] X. Y. Liu, P. L. Wang, Y. J. Shen, S. Y. Bi, W. Ren and D. S. Zhang, Boosting SO_2-Tolerant Catalytic Reduction of NO_x via Selective Adsorption and Activation of Reactants over Ce^{4+}-SO_4^{2-} Pair Sites, ACS Catal., 2022, 12, 11306-11317.

[38] L. Zhang, L. Zhang, G. C. Xu, C. Zhang, X. Li, Z. P. Sun and D. Z. Jia, Low-temperature CO oxidation over CeO_2 and $CeO_2@Co_3O_4$ core-shell microspheres, New J. Chem. 2017, 41, 13418.

[39] H. X. Mai, L. D. Sun, Y. W. Zhang, R. Si, W. Feng, H. P. Zhang, H. C. Liu and C. H. Yan, Shape-Selective Synthesis and Oxygen Storage Behavior of Ceria Nanopolyhedra, Nanorods, and Nanocubes, J. Phys. Chem. B, 2005, 109, 24380-24385.

[40] O. A. Shilova, A. M. Nikolaev, A. S. Kovalenko, A. A. Sinel'nikov, K. E. Yorov, N. V. Tsvigun, V. V. Volkov, T. V. Khamova, G. G. Panova and G. P. Kopitsa, Aqueous chemical synthesis of iron oxides

magnetic nanoparticles of different morphology and mesostructured, Ceram. Int., 2021, 47, 28866-28873.

[41] X. H. Zheng, Y. L. Li, L. Y. Zhang, L. J. Shen, Y. H. Xiao, Y. F. Zhang, C. T. Au and L. L. Jiang, Insight into the effect of morphology on catalytic performance of porous CeO_2 nanocrystals for H_2S selective oxidation, Appl. Catal., B, 2019, 252, 98-110.

[42] G. Y. Mu, Y. Zeng, Y. Zheng, Y. N. Cao, F. J. Liu, S. J. Liang, Y. Y. Zhan and L. L. Jiang, Oxygen vacancy defects engineering on Cu-doped Co_3O_4 for promoting effective COS hydrolysis, Green Energy Environ. 2023, 8, 831-841.

[43] S. Loridant, Raman spectroscopy as a powerful tool to characterize ceria-based catalysts, Catal. Today, 2021, 373. 98-111.

[44] D. Liu, F. Y. Hu, Y. Yan, R. P. Ye, X. H. Chen, B. Y, Han, Z. H. Lu, L. Zhou, G. Feng and R. B. Zhang, Promotion of oxygen vacancies and metal-support interaction over 3DOM Au/CeO_2 catalyst for CO oxidation, Appl. Surf. Sci., 2023, 629, 157438.

[45] J. Mei, Y. Ke, Z. J. Yu, X. F. Hu, Z. Qu and N. Q. Yan, Morphology-dependent properties of Co_3O_4/CeO_2 catalysts for low temperature dibromomethane (CH_2Br_2) oxidation, Chem. Eng. J., 2017, 320, 124-134.

[46] G. D. Zhang, X. S. Huang and Z. C. Tang, New insight into the synergistic promotion effect of phosphorus and molybdenum on the ceria-titanium catalysts for superior SCR performance, Mol. Catal., 2019, 478, 110562.

[47] Z. B. Xiong, W. Wang, J. Li, L. H. Huang and W. Lu, The synergistic promotional effect of W doping and sulfate modification on the NH_3-SCR activity of CeO_2 catalyst, Mol. Catal., 2022, 522, 112250.

[48] W. P. Shan, F. D. Liu, H. He, X. Y. Shi and C. B. Zhang, A superior Ce-W-Ti mixed oxide catalyst for the selective catalytic reduction of NO_x with NH_3, Appl. Catal., B, 2012, 115-116, 100-106.

[49] S. J. Hu, J. N. Gu, K. Li, J. X. Liang, Y. X. Xue, X. Min, M. M. Guo, X. F. Hu, J. P. Jia and T. H. Sun, Boosting COS catalytic hydrolysis performance over Zn-Al oxide derived from ZnAl hydrotalcite-like compound modified via the dopant of rare earth metals and the replacement of precipitation base, Appl. Surf. Sci., 2022, 599, 154016.

[50] W. X. Zhao, J. Rong, W. Luo, L. L. Long and X. J. Yao, Enhancing the K-poisoning resistance of CeO_2-SnO_2 catalyst by hydrothermal method for NH_3-SCR reaction, Appl. Surf. Sci., 2022, 579, 152176.

[51] P. Zhang, A. L. Chen, T. W. Lan, X. Y. Liu, T. T. Yan, W. Ren and D. S. Zhang, Balancing acid and redox sites of phosphorylated CeO_2 catalysts for NO_x reduction: The promoting and inhibiting mechanism of phosphorus, J. Hazard. Mater., 2023, 441, 129867.

[52] D. K. Chen, D. D. He, J. C. Lu, L. P. Zhong, F. Liu, J. P. Liu, J. Yu, G. P. Wan, S. F. He and Y. M. Luo, Investigation of the role of surface lattice oxygen and bulk lattice oxygen migration of cerium-based oxygen carriers: XPS and designed H_2-TPR characterization, Appl. Catal., B, 2017, 218, 249-259.

[53] D. D. Ma, D. K. Sun, Y. J. Zou, S. M. Mao, Y. X. Lv, Y. Wang, J. Li, J. W. Shi, The synergy between electronic anchoring effect and internal electric field in CdS quantum dots decorated dandelion-like Fe-CeO_2 nanoflowers for improved photocatalytic hydrogen evolution, J. Colloid and Interface Sci., 2019, 549, 179-188.

[54] A. Younis, D. Chu, Y. V. Kaneti and S. Li, Tuning the surface oxygen concentration of {111} surrounded ceria nanocrystals for enhanced photocatalytic activities, Nanoscale, 2016, 8, 378.

[55] J. Li, F. Zhou, Z. B. Xiong, Y. P. Du, Q. G. Yang, W. Wang and W. Lu, Promotional Effect of Zirconium Doping on the NH_3-SCR Activity of CeO_2 and CeO_2-TA Modified by Thiourea: A Comparative Study, ChemCatChem, 2023, 15, e202201578.

[56] C. Fang, L. Y. Shi, H. R. Li, L. Huang, J. P. Zhang and D. S. Zhang, Creating hierarchically macro-/mesoporous Sn/ CeO_2 for the selective catalytic reduction of NO with NH_3, RSC Adv., 2016, 6, 78727.

[57] L. Huang, Y. Q. Zeng, Y. B. Gao, H. Wang, Y. H. Zong, Z. F. Chang, S. L. Zhang, P. Han and Y. Yu, Promotional effect of phosphorus addition on improving the SO_2 resistance of V_2O_5-MoO_3/TiO_2 catalyst for NH_3-SCR of NO, J. Phys. Chem. Solids, 2022, 163, 110566.

[58] X. B. Wang, R. B. Duan, W. Liu, D. W. Wang, B. R. Wang, Y. R. Xu, C. H. Niu, J. W. Shi, The insight into the role of CeO_2 in improving low-temperature catalytic performance and SO_2 tolerance of $MnCoCeO_x$ microflowers for the NH_3-SCR of NO_x, Appl. Surf. Sci., 2020, 510, 145517.

[59] H. K. Jin, Z. Y. An, Q. C. Li, Y. Q. Duan, Z. H. Zhou, Z. K. Sun and L. B. Duan, Catalysts of Ordered Mesoporous Alumina with a Large Pore Size for Low-Temperature Hydrolysis of Carbonyl Sulfide, Energy Fuels, 2021, 35, 8895-8908.

[60] P. Ning, L. L. Yu, H. H. Yi, X. L. Tang, H. Li, H. Y. Wang and L. N. Yang, Effect of Fe/Cu/Ce loading on the coal-based activated carbons for hydrolysis of carbonyl sulfide, J. Rare Earths, 2010, 28, 205.

[61] J. J. Zou, S. Impeng, F. L. Wang, T. W. Lan, L. L. Wang, P. L. Wang and D. S. Zhang, Compensation or Aggravation: Pb and SO_2 Copoisoning Effects over Ceria-Based Catalysts for NO_x Reduction, Environ. Sci. Technol., 2022, 56, 13368-13378.

[62] X. Li, X. Q. Wang, L. L. Wang, L. Yuan, Y. X. Ma, Y. B. Xie, Y. R. Xiong and P. Ning, Alkali-induced metal-based coconut shell biochar for efficient catalytic removal of H_2S at a medium–high temperature in

blast furnace gas with significantly enhanced S selectivity, Sep. Purif. Technol, 2023, 306, 122698.

[63] X. X. Wu, V. Schwartz, S. H. Overbury and T. R. Armstrong, Desulfurization of Gaseous Fuels Using Activated Carbons as Catalysts for the Selective Oxidation of Hydrogen Sulfide, Energy Fuels, 2005, 19, 1774-1782.

[64] L. Zhang, W. X. Zou, K. L. Ma, Y. Cao, Y. Xiong, S. G. Wu, C. J. Tang, F. Gao and L. Dong, Sulfated Temperature Effects on the Catalytic Activity of CeO_2 in NH_3-Selective Catalytic Reduction Conditions, The Journal of Physical Chemistry C, 2015, 119, 1155-1163.

[65] W. P. Shan, Y. Geng, X. L. Chen, N. Huang, F. D. Liu and S. J. Yang, A highly efficient $CeWO_x$ catalyst for the selective catalytic reduction of NO_x with NH_3, Catal. Sci. Technol., 2016, 6, 1195.

[66] Z. C. Chen, S. Ren, Y. H. Zhou, X. D. Li, M. M. Wang and L. Chen, Comparison of Mn doped CeO_2 with different exposed facets for NH_3-SCR at low temperature, J. Energy Inst., 2022, 105, 114-120.

[67] J. Yang, S. Ren, T. S. Zhang, Z. H. Su, H. M. Long, M. Kong, L. Yao, Iron doped effects on active sites formation over activated carbon supported Mn-Ce oxide catalyst for low-temperature SCR of NO, Chem. Eng. J, 2020, 379, 122398.

[68] J. Arfaoui, A. Ghorbel, C. Petitto, G. Delahay, Effect of acidic components (SO_4^{2-} and WO_3) on the surface acidity, redox ability and NH_3-SCR activity of new CeO_2-TiO_2 nanoporous aerogel catalysts: A comparative study, Inorg. Chem. Commun, 2022, 140, 109494.

[69] P. Zhang, R. T. Guo, L. J. Wu and W. G. Pan, The enhancement of NH_3-SCR performance for CeO_2 catalyst by CO pretreatment, Environ. Sci. Pollut. Res., 2020, 27, 13617-13636.

[70] K. L. Song, K. Y. Guo, Y. X. Lv, D. D. Ma, Y. H. Cheng, J. W. Shi, Rational Regulation of the Reducibility and Acid Site on Mn-Fe-BTC to Achieve High Low-Temperature Catalytic Denitration Performance, ACS Appl. Mater. Interfaces, 2023,15,4132-4143.

[71] Z. H. Wu, Y. Q. Zeng, F. J. Song, S. L. Zhang, and Q. Zhong， Active sites assembly effect on CeO_2-WO_3-TiO_2 catalysts for selective catalytic reduction of NO with NH_3, Mol. Catal., 2019, 479, 110549.

[72] J. Tang, L. K. Zhao, S. Jiang, Y. Huang, J. F. Zhang and J. Li, Effect of Transition-Metal Oxide M (M=Co, Fe, and Mn) Modification on the Performance and Structure of Porous CuZrCe Catalysts for Simultaneous Removal of NO and Toluene at Low-Medium Temperatures, Energy Fuels， 2022, 36, 4439-4455.